

APPLICATIONS AND TECHNOLOGY

STAND FOR RF GAP BREAKDOWN STRENGTH STUDY IN MAGNETIC FIELD

P.A. Demchenko, Eu.V. Gushev, N.G. Shulika, O.N. Shulika, D.Yu. Zalesky
National Science Center "Kharkov Institute of Physics and Technology", Kharkov, Ukraine
E-mail: demchenko@kipt.kharkov.ua

Presented are the design and the features of the stand for experimental studies of high-frequency gap electric strength in a magnetic field along with the verification of magnetic circuit simulation of linac accelerating structure with combined alternating-phase and magnetic focusing.

PACS: 29.20.Ej

INTRODUCTION

The means to enhance stability of proton beam focusing in a linear resonance accelerator with alternating-phase focusing are under study at the Institute of Plasma Electronics and New Acceleration Methods of NSC KIPT. It is well known that there exists a very strong connection between longitudinal and transverse particle dynamics in linac accelerating channels with alternating-phase focusing. As a result, effective beam emittance increases leading to current losses and activation of linac structural units [1].

To increase the effect of proton beam focusing by RF electric field and, therefore, to decrease an amplitude of particle radial oscillations in an accelerating channel, it is proposed to apply an external magnetic field in gaps between drift tubes [1].

There are several ways how to produce a longitudinal magnetic field in accelerating gaps between axial-symmetric drift tubes. One of them is to use tubes made of ferromagnetic material with high saturation induction. An outer shell of the tubes is made of copper. The thickness of the shell should exceed the skin-layer thickness at operation frequency to preserve resonator Q-factor of accelerating structure. As this takes place, the RF power supply of linac does not change.

A sequence of the drift tubes with ferromagnetic core forms a magnetic circuit where magnetic field is concentrated in accelerating gaps between the tubes. To lessen dissipation of magnetic induction flux along the drift tubes, it is important to ensure the ferromagnetic material is not in the saturation mode and possesses high relative magnetic permeability μ_r . It is clear that maximum induction in a gap is always less than saturation induction of a drift tube material.

Thus, the drift tubes have two functions: on the one hand they serve as electrodes with voltage difference to accelerate charged particles, and on the other hand they serve as magnetic poles for additional particle beam magnetic focusing. Fig. 1 illustrates a conceptual version of a section with combined alternating-phase and magnetic focusing [1].

The magnetic circuit is formed by the drift tube sequence and the yoke system with a coil to provide magnetic flux Φ , see Fig. 1. The coil is outside the vacuum chamber with the accelerating structure.

The above design of an accelerating channel with combined focusing was named a *structure with spatially combined alternating-phase and magnetic focusing*.

Such structures can be used to accelerate proton beams in low and medium energy range (up to 100 MeV).

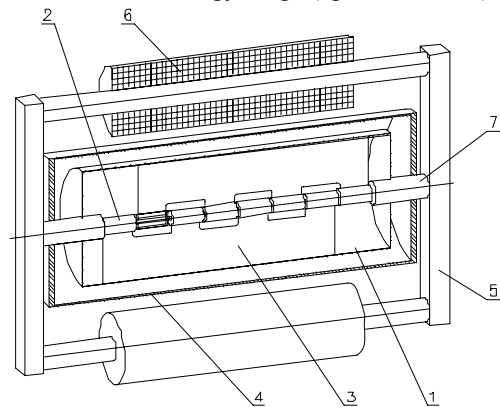


Fig. 1. Section with combined alternating-phase and magnetic focusing: 1 – resonator; 2 – drift tube; 3 – rack; 4 – vacuum chamber; 5 – magnetic conductor; 6 – coil; 7 – pole tip

EXPERIMENTAL STAND FOR STUDIES OF RF GAP BREAKDOWN STRENGTH IN MAGNETIC FIELD

The development of an accelerating section with spatially combined alternating-phase and magnetic focusing, see Fig. 1, calls for preliminary scientific R&D work. In particular, it is important to perform magnetic circuit simulation for accelerating gap flux density evaluation in a resonant section. The magnetic circuit requirements are specified after charged particle dynamics simulation. As a result of the magnetic circuit simulation, it is expected the following problems will be resolved:

- the design and materials for the magnetic circuit including drift tubes;
- the coil parameters and design;
- the coil power supply;
- coil heat generation problem and cooling;
- magnitude of magnetic ponderomotive force that affects accelerating section elements made of ferromagnetic materials;
- necessary mechanical stiffness of an accelerating section considering its deformation as a result of magnetic field affect.

It is very important to investigate the electric strength of RF accelerating gaps when magnetic field generated by drift tubes with ferromagnetic core is applied. Electric field intensity in gaps defines the maximal accelerating rate.

To solve these problems, an experimental stand is being designed. Also, the stand is being used for simulation results verification. For the R&D cost reduction, a simple construction of a resonant accelerating section has been considered.

As the result of numerical simulation, the section with two drift tubes and one accelerating gap between them has been chosen as a test model. Low-carbon steel (Stee 13, Stee 110) has been selected as ferromagnetic material for magnetic circuit elements. In preliminary

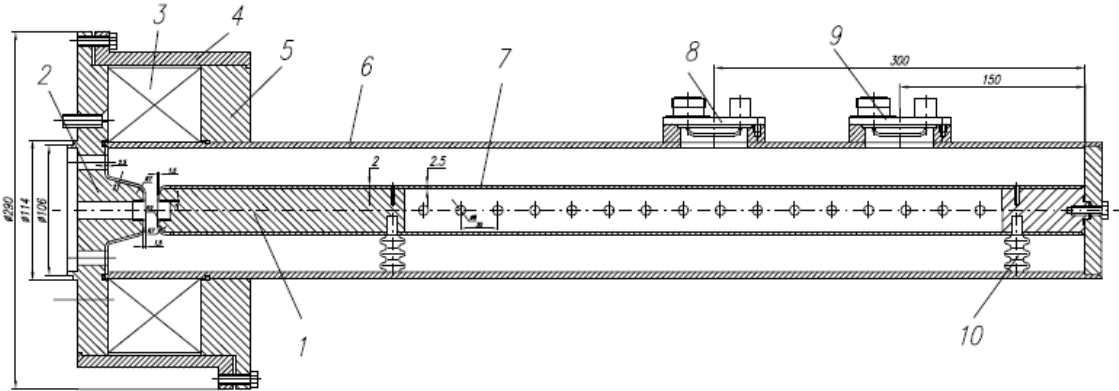


Fig. 2. Experimental stand for RF breakdown strength studies in magnetic field: 1, 2 – ferromagnetic poles/electrodes; 3 – coil; 4, 5 – magnetic shields; 6, 7 – coaxial resonator electrodes; 8, 9 – coupling loops; 10 – insulator

The coaxial parts of the resonator are formed by copper cylindrical tubes 6 and 7. The interior volume of the tube 7 is partially filled with ferromagnetic material thus forming the ferromagnetic core of electrode 1. The electrode 1 face is covered with copper layer 1 mm thick. The electrode 2 is made of ferromagnetic material and has 1 mm thick copper coating on the resonator side. Conditions on copper surface of the electrodes 1 and 2 should meet the technological requirements for drift tube surfaces in present-day linacs.

Thus, the electrodes 1 and 2 form an RF electric field in the gap between them as well as create a focusing magnetic field.

The closed magnetic circuit consists of the pole/electrode 1, the accelerating gap, the pole/electrode 2, the cylindrical magnetic yokes 4,5 and the circular vacuum gap between the magnetic core 5 and the pole/electrode 1. Magnetic potential difference between the poles is produced by the coil 3.

The coupling loops 8 and 9 provide high-frequency electromagnetic field excitation in the resonator. The coaxial electrode 7 is centered by the insulators 10 installed in group of three at an angle of 120° in each resonator cross-section.

The stand is connected with the vacuum volume through a flange where the pole 2 is installed. Pumping occurs through apertures in the flange and the channel along the axis, see Fig. 2. Axial apertures in the electrodes 1 and 2 simulate a channel for ion beam passing. Residual gas pressure in the chamber is $1.3 \cdot 10^{-4}$ Pa.

Numerical simulation of the magnetic circuit presented in Fig. 2 is performed using FEMM code, version 4.2. This software is based on the finite element method [2] which allows one to calculate field distribution for plane and axial-symmetric geometries using

experiments, the magnetically soft steel has been used as the drift tube core material. In further experiments, it is supposed to replace the steel with an iron-cobalt alloy (*permdure*) due to its high saturation induction up to 2.2 T to increase magnetic field induction in a gap.

The stand design is presented in Fig. 2. The accelerating structure is a quarter-wave coaxial resonator operating at a frequency $f=100$ MHz. The electrodes 1 and 2 form the accelerating gap at the cut-section of central electrode. The coaxial resonator length is 760 mm.

magnetization (B-H) curves for different ferromagnetic materials.

The solution method for magnetostatics problems is based on calculation of magnetic field vector potential \vec{A} connected with field induction \vec{B} by the relation $\vec{B} = \text{rot } \vec{A}$.

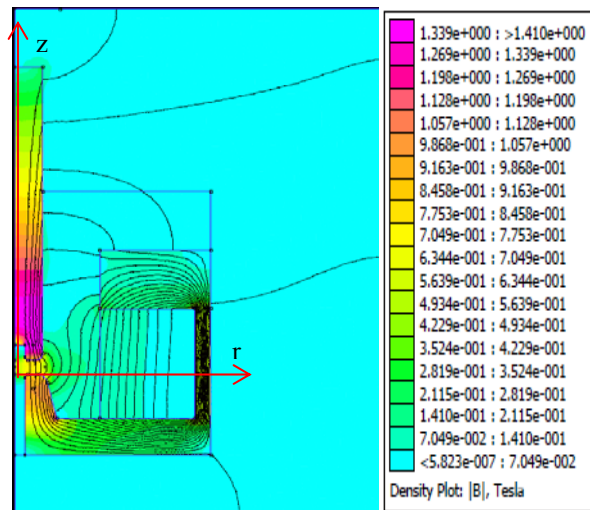


Fig. 3. Magnetic field topography in a quarter-wave coaxial resonator

On the other hand, vector potential satisfies Poisson equation $\Delta \vec{A} = -\mu \vec{j}$. Here $\vec{j}(r,z)$ is distribution of electric current inducing magnetomotive force, $\mu(r,z)$ is magnetic permeability, r,z are radial and axial coordinates respectively.

In axial-symmetrical geometry, vector potential has only one component $A(r,z)$ normal to (r,z) -plane and obeys Laplace equation $\Delta A=0$.

Fig. 3. represents the distribution of magnetic field induced by the coil with magnetomotive force of 8000 ampere-turn. Absolute values of magnetic induction are shown in color spectrum.

As it follows from the numerical simulation, see Fig. 3, magnetic induction on the poles of accelerating gap is less than 0.96 T. It results from low saturation induction in steel $B_s \approx 1.4$ T. Referring to Fig. 3, it is clear that a part of electrode 2 ferromagnetic core is near saturation.

If we use supermendur 49K2ΦA as a material for poles 1 and 2 then surface induction could be increased up to 1.2...1.3 T.

The distribution of magnetic induction $|B|$ between the accelerating gap poles along z-axis at $r=18$ mm is illustrated in Fig. 4. At this radius the maximal induction is observed at corresponding points on the pole surfaces. The poles are round-shaped to decrease both electric and magnetic field gradients along the surface.

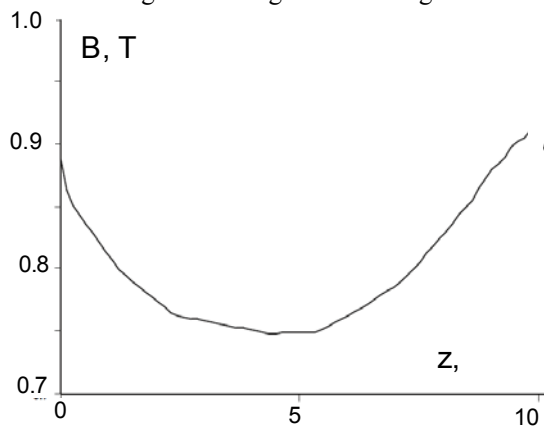


Fig. 4. Longitudinal distribution of magnetic induction between poles at $r=18$ mm

As it follows from Fig. 4, magnetic induction at the outer pole 2 is about $B_2 \approx 0.85$ T, then it declines monotonously to about 0.75 T in the middle plane of the accelerating gap forming a so-called field dip and then increases again up to about $B_1 \approx 0.96$ T at the inner pole 1. Non-symmetry in the curve behavior is due to the different pole geometry. Attractive force that acts on the inner electrode 1 is 450 H.

In order to obtain presented magnetic induction values, it is required about 800 W power supply for the coil.

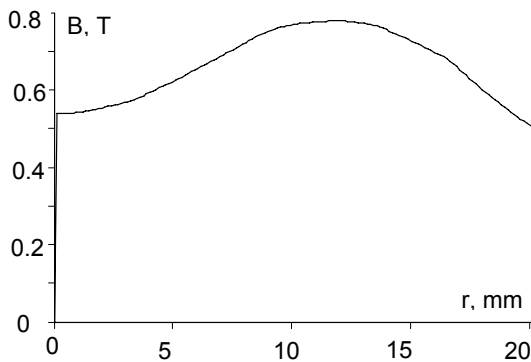


Fig. 5. Radial magnetic induction distribution in the middle plane between the electrodes

Fig. 5 presents the radial distribution of magnetic induction $|B|$ in the middle plane between the poles. The maximal induction value is about 0.8 T. The field dip on the axis is caused by the pole apertures used to simulate the channel for the ion beam transportation.

An important problem for an accelerating structure with spatially combined alternating-phase and magnetic focusing is electrical strength of vacuum gaps. When a large magnetic field is applied between electrodes the electric breakdown probability may increase. Electrical strength could depend on magnetic induction and field topography in an accelerating gap.

In present-day technique of charged particle linacs, Kilpatrick criterion giving the relationship between a field frequency f and an electric intensity E on electrodes is used to evaluate the possibility of electrical breakdown without magnetic field [3]. In case of copper electrodes this criterion is $f=1.64 \cdot E_K^2 \cdot \exp(-8.5/E_K)$, where f is field frequency (MHz); E_K is maximal electric field intensity that provides stable operation mode without breakdown of drift tube gaps (MV/m) [4].

It should be emphasized that Kilpatrick criterion depends on several empiric parameters based on experiments. An excess factor at E_k depends on electrode surface roughness, electrode contamination, vacuum conditions, etc. Under modern technology conditions it could reach up to 1.2...2 depending on electrode manufacturing process and vacuum hygiene [4].

To induce an electric field between poles 1 and 2 (see Fig. 2), an external RF generator is used to excite oscillations in the resonator at a frequency $f_0=100$ MHz.

During numerical simulation the following parameters have been calculated: a resonator Q-factor, electric field distribution in the gap at the storage energy $W_0=1$ J, RF power needed to obtain electric fields which are equal to or exceed Kilpatrick criterion.

It follows from the calculation analyses that the resonator Q-factor is about $Q \approx 3500$ if the resonator and electrode copper surfaces and element junctions have no defects.

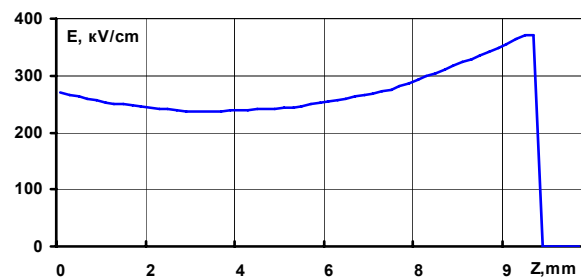


Fig. 6. Longitudinal distribution of electric field intensity in gap between electrodes at $r=18$ mm and storage resonator energy 1 J

Fig. 6. shows the distribution of electric intensity between the electrodes along z-axis at $r=18$ mm for the storage resonator energy $W_0=1$ J. As this takes place, electric field intensity reaches about $E_{max} \approx 360$ kV/cm on the inner electrode surface while on the surface of the outer electrode its value is about 260 kV/cm. The difference is due to the difference in the electrode geometry which has been optimized to obtain magnetic field induction in the gap as high as possible.

Fig. 7 presents the radial distributions of the electric field intensity $|E|$ at tangential planes of the inner (1) and outer (2) electrodes for the same storage resonator energy $W_0=1$ J. Again, the difference between two distributions is a result of the electrode geometry difference.

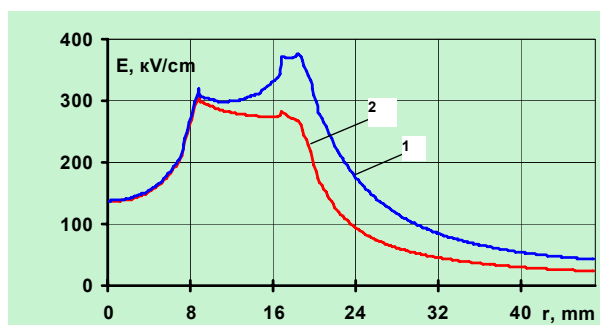


Fig. 7. Radial distribution of electric field intensity at inner (1) and outer (2) electrodes

Kilpatrick criterion in case of copper electrodes and field frequency $f_0=100$ MHz is $E_K \approx 110$ kV/cm. Considering that $Q = 2\pi f_0 W_0 / P_{dis}$ (where f_0 is a resonator frequency, W_0 is storage resonator energy, P_{dis} is power dissipated in the resonator), a power supply $P_{dis} \approx 180$ kW is required to generate an electric field with intensity $E_{max} \approx 360$ kV/cm at $W_0=1$ J. Since power dissipation is proportional to electric field intensity squared E^2 , an RF generator with power about 20 kW is sufficient to meet Kilpatrick criterion conditions.

At present, an RF generator with the following parameters: output capacity up to 400 kW, pulse duration 200 μ s, pulse repetition up to 10 Hz is available to the stand developers.

CONCLUSIONS

Based on results of simulation, the design and construction documentation of the stand for experimental studies of high-frequency gap electric strength in a magnetic field has been developed. The stand will also be used for the verification of the results of magnetic circuit simulation for proton linac sections with combined alternating-phase and magnetic focusing.

REFERENCES

1. S.A. Vdovin, P.A. Demchenko, Ye.V. Gussev, M.G. Shulika, O.M. Shulika. Combined Focusing in Linear Ion Accelerator // *Problems of Atomic Science and Technology. Series "Plasma Electronics and New Methods of Acceleration"* (68). 2010, № 4, p. 325-329.
2. D. Meeker. Finite Element Method Magnetics FEMM 4.2, User's Manual, 2010, 158 p. (<http://www.femm/info>).
3. W.D. Kilpatrick. Criterion for Vacuum Sparking Designed to Include RF and DC // *Rev. Sci. Instrum.* 1957, v. 28. p. 824-826.
4. T.P. Wangler. *RF Linear Accelerators*. Wiley-VCH, 2008, 450 p.

Article received 04.03.2013.

СТЕНД ДЛЯ ИССЛЕДОВАНИЙ ЭЛЕКТРИЧЕСКОЙ ПРОЧНОСТИ ВЧ-ЗАЗОРОВ В МАГНИТНОМ ПОЛЕ

П.А. Демченко, Е.В. Гусев, Н.Г. Шулика, О.Н. Шулика, Д.Ю. Залеский

Приведены конструкция и характеристики стенда для экспериментальных исследований электрической прочности высокочастотных зазоров в магнитном поле и проверки результатов численного моделирования магнитных цепей ускоряющих структур линейных ускорителей с комбинацией переменного-фазовой и магнитной фокусировок.

СТЕНД ДЛЯ ДОСЛІДЖЕНЬ ЕЛЕКТРИЧНОЇ МІЦНОСТІ ВЧ-ЗАЗОРІВ У МАГНІТНОМУ ПОЛІ

П.О. Демченко, Є.В. Гусев, М.Г. Шуліка, О.М. Шуліка, Д.Ю. Залеський

Надано конструкцію та характеристики стенду для експериментальних досліджень електричної міцності високочастотних зазорів у магнітному полі та перевірки результатів чисельного моделювання магнітного кола прискорювальних структур лінійних прискорювачів з комбінацією змінно-фазового і магнітного фокусування.